

# Efficient shortcuts to adiabatic passage for the fast populations transfer in multiparticle systems

Ye-Hong Chen<sup>1</sup>, Qing-Qin Chen<sup>2</sup>, Yan Xia<sup>1,\*</sup>, and Jie Song<sup>3,†</sup>

<sup>1</sup>*Department of Physics, Fuzhou University, Fuzhou 350002, China*

<sup>2</sup>*Zhicheng College, Fuzhou University, Fuzhou 350002, China*

<sup>3</sup>*Department of Physics, Harbin Institute of Technology, Harbin 150001, China*

Achieving fast population transfer (FPT) in multiparticle systems based on the cavity quantum electronic dynamics is an outstanding challenge. In this paper, motivated by the quantum Zeno dynamics, a shortcut for performing the FPT of ground states in multiparticle systems with the invariant based inverse engineering is proposed. Numerical simulation demonstrates that a perfect population transfer of ground states in multiparticle systems can be rapidly achieved in one step, and the FPT is robust to both the cavity decay and atomic spontaneous emission. Additionally, this scheme is not only implemented without requiring extra complex conditions, but also insensitive to variations of the parameters.

PACS numbers: 03.67. Pp, 03.67. Mn, 03.67. HK

Keywords: Fast populations transfer; Invariant-based inverse engineering; Multiparticle system

## I. INTRODUCTION

Reliable population transfer of a quantum system with time-dependent interacting fields has become a significant ingredient in the quantum information processing for various applications ranging from quantum storage to quantum communication [1–4]. It has already drawn great attention in recent years [5, 6]. Several approaches have been proposed for attaining complete population transfers with different methods, including  $\pi$  pulses, composite pulses, rapid adiabatic passage (RAP), stimulated Raman adiabatic passage (STIRAP),

---

\* E-mail: xia-208@163.com

† E-mail: jsong@hit.edu.cn

and their variants [2–4]. However, most of them have some shortcomings, say,  $\pi$  pulses is fast yet highly sensitive to variations in the pulse area, and to inhomogeneities in the sample [7], the adiabatic passage technique is robust versus variations in the experimental parameters while it usually needs a relatively long interaction time. If the required evolution time is too long, the scheme may be useless, because decoherence would spoil the intended dynamics. Therefore, accelerating the dynamics towards the perfect final outcome is a good idea and perhaps the most reasonable way to actually fight against the decoherence that is accumulated during a long operation time.

Recently, a lot of work has been done in finding shortcuts to adiabaticity for the two- or three-level atomic system [8–15]. By means of resonant laser pulses, Chen and Muga have successfully performed fast population transfer (FPT) in three-level systems via invariant-based inverse engineering [13]. A quantum computation network has long been thought to partition into a sequence of one-qubit rotations and two-qubit gates [16]. Nevertheless, it is too large to construct a quantum computation network to perform computation by decomposing into one-qubit rotations and two-qubit gates. So, the FPT in a multiparticle system is a fundamental operation for scalable quantum information processors. However, it is a pity that most of the previous studies based on the invariant-based inverse engineering for achieving FPTs are in two- or three-level single-atom systems, and it is very hard to directly design a model for the FPT in multiparticle systems. Until recently, Lu *et al.* have proposed a scheme to implement the quantum state transfer between two three-level atoms based on the invariant-based inverse engineering in the cavity quantum electronic dynamics (QED) system [17]. They sent two atoms through the cavity with a short time interval, and the atoms suffered the opposite variation tendency in the time-dependent laser pulse and atom-cavity coupling. Through designing related parameters and controlling the time interval between the two atoms sent through the cavity, they effectively implemented ultrafast quantum state transfer between two  $\Lambda$ -type atoms. Reference [17] successfully introduced shortcuts to adiabatic passage into cavity QED systems. However, Ref. [17] is limited by the following: (i) Only quantum state transfer in a two-atom system could be realized. When it comes to more complex systems, for example, multiparticle systems, cavity coupling systems, and cavity-fiber-atom combined systems, this scheme is useless; new designs are required in a different situation. (ii) Sequential operations were needed in a two atoms system; this may eliminate the possibility of success in experiment.

On the other hand, the quantum Zeno effect which has been tested in many experiments is the inhibition of transitions between quantum states by frequent measurements [18–21]. The system can actually evolve away from its initial state while it still remains in the so-called Zeno subspace determined by the measurement when frequently projected onto a multi-dimensional subspace. This was called “quantum Zeno dynamics” by Facchi and Pascazio in 2002 [22]. And quantum Zeno dynamics (QZD) can be achieved via continuous coupling between the system and an external system instead of discontinuous measurements. In general, we assume that a dynamical evolution process is governed by the Hamiltonian  $H_K = H_{obs} + KH_{meas}$ , where  $H_{obs}$  is Hamiltonian of the quantum system investigated,  $K$  is a coupling constant, and  $H_{meas}$  is viewed as an additional interaction Hamiltonian performing the measurement. In the limit  $K \rightarrow \infty$  the system will remain in the same Zeno subspace as that of its initial state. The evolution operator is described as  $U(t) = \exp(-it \sum_n K \eta_n P_n + P_n H_{obs} P_n)$ , with  $P_n$  being the eigenvalue projection of  $H_{meas}$  with eigenvalues  $\eta_n$  ( $H_{meas} = \sum_n \eta_n P_n$ ).

To more widely generalize the efficiency and application of the FPT in multiparticle systems based on shortcuts to adiabatic passage in cavity QED systems, motivated by the space division of QZD, we propose an effective method by invariant-based inverse engineering. Compared with previous works, this protocol has the following advantages. First, the fast population transfer in a multiparticle system can be achieved in one step. Secondly, the shortcut to the adiabatic passage is reliable for dealing with much more complex situations, for example, multiparticle systems, cavity coupling systems, and cavity-fiber-atom combined systems.

The paper is structured as follows. In Sec. II, we construct a shortcut passage for FPT in a system with two  $\Lambda$ -type atoms trapped in a cavity. A resonant time-dependent laser pulse and a resonant ordinary atom-cavity coupling are applied to each atom. In Sec. III, we analyze the feasibility of the FPT in multiparticle systems based on the shortcut proposed in Sec. II. Sec. IV is the conclusion.

## II. SHORTCUTS TO ADIABATIC PASSAGE FOR THE FAST POPULATIONS TRANSFER IN TWO-ATOM SYSTEM

As shown in Fig. 1, we consider that two  $\Lambda$ -type atoms 1 and 2 are trapped in a cavity  $c$ . Each atom has an excited state  $|e\rangle$  and two ground states  $|f\rangle$  and  $|g\rangle$ . The atomic transition  $|f\rangle \leftrightarrow |e\rangle$  is resonantly driven through a time-dependent laser pulse with Rabi frequency  $\Omega(t)$ , and the transition  $|g\rangle \leftrightarrow |e\rangle$  is resonantly coupled to the cavity mode with coupling constant  $\lambda$ . The whole Hamiltonian in the interaction picture is written as

$$\begin{aligned} H_I &= H_{al} + H_{ac}, \\ H_{al} &= \sum_{k=1,2} \Omega_k(t) |e\rangle_k \langle f| + H.c., \\ H_{ac} &= \sum_{k=1,2} \lambda_k |e\rangle_k \langle g| a + H.c., \end{aligned} \quad (1)$$

where subscript  $k$  denotes the  $k$ th atom, and  $a$  is the annihilation operator for the cavity. If the initial state is  $|\psi_0\rangle = -|f\rangle_1 |g\rangle_2 |0\rangle_c$ , the whole system evolves in the subspace spanned by

$$\begin{aligned} |\psi_1\rangle &= |f\rangle_1 |g\rangle_2 |0\rangle_c, \\ |\psi_2\rangle &= |e\rangle_1 |g\rangle_2 |0\rangle_c, \\ |\psi_3\rangle &= |g\rangle_1 |g\rangle_2 |1\rangle_c, \\ |\psi_4\rangle &= |g\rangle_1 |e\rangle_2 |0\rangle_c, \\ |\psi_5\rangle &= |g\rangle_1 |f\rangle_2 |0\rangle_c. \end{aligned} \quad (2)$$

In light of QZD, we rewrite the Hamiltonian in Eq. (1) with the eigenvectors of  $H_{ac}$  (we set  $\lambda_1 = \lambda_2 = \lambda$ ),

$$\begin{aligned} |\phi_1\rangle &= \frac{1}{\sqrt{2}} (-|\psi_2\rangle + |\psi_4\rangle), \\ |\phi_2\rangle &= \frac{1}{2} (|\psi_2\rangle + \sqrt{2}|\psi_3\rangle + |\psi_4\rangle), \\ |\phi_3\rangle &= \frac{1}{2} (|\psi_2\rangle - \sqrt{2}|\psi_3\rangle + |\psi_4\rangle), \end{aligned} \quad (3)$$

with eigenvalues  $E_1 = 0$ ,  $E_2 = \sqrt{2}\lambda$ , and  $E_3 = -\sqrt{2}\lambda$ . We obtain

$$H'_I = H'_{al} + H'_{ac},$$

$$\begin{aligned}
H'_{ac} &= \sum_{n=1}^3 E_n |\phi_n\rangle \langle \phi_n|, \\
H'_{al} &= \frac{\Omega_1(t)}{\sqrt{2}} (-|\phi_1\rangle \langle \psi_1|) + \frac{\Omega_1(t)}{2} |\phi_2\rangle \langle \psi_1| + \frac{\Omega_1(t)}{2} |\phi_3\rangle \langle \psi_1| + \frac{\Omega_2(t)}{\sqrt{2}} |\phi_1\rangle \langle \psi_5| \\
&\quad + \frac{\Omega_2(t)}{2} |\phi_2\rangle \langle \psi_5| + \frac{\Omega_2(t)}{2} |\phi_3\rangle \langle \psi_5| + H.c..
\end{aligned} \tag{4}$$

It is obvious that there are four non-zero energy eigenvalues  $\pm\Omega_1(t)$  and  $\pm\Omega_2(t)$  for the Hamiltonian  $H'_{al}$ . Therefore, setting  $\sqrt{2}\lambda \gg \Omega_k(t)$ , the condition  $H'_{ac} \gg H'_{al}$  and the Zeno condition  $K \rightarrow \infty$  are satisfied ( $H'_{al}$  and  $H'_{ac}$  correspond to  $H_{obs}$  and  $KH_{meas}$  in Sec. I, respectively). Performing the unitary transformation  $U = e^{-iH'_{ac}t}$  under condition  $H'_{ac} \gg H'_{al}$ , we obtain

$$\begin{aligned}
H_{al}^{eff} &= \frac{\Omega_1(t)}{\sqrt{2}} (-|\phi_1\rangle \langle \psi_1|) + \frac{\Omega_1(t)}{2} (e^{i\sqrt{2}\lambda t} |\phi_2\rangle \langle \psi_1|) + \frac{\Omega_1(t)}{2} (e^{-i\sqrt{2}\lambda t} |\phi_3\rangle \langle \psi_1|) + \frac{\Omega_2(t)}{\sqrt{2}} (|\phi_1\rangle \langle \psi_5|) \\
&\quad + \frac{\Omega_2(t)}{2} (e^{i\sqrt{2}\lambda t} |\phi_2\rangle \langle \psi_5|) + \frac{\Omega_2(t)}{2} (e^{-i\sqrt{2}\lambda t} |\phi_3\rangle \langle \psi_5|) + H.c..
\end{aligned} \tag{5}$$

The terms with the oscillating frequency  $\sqrt{2}\lambda$  are possible to be ignored in the present case. And the Hilbert subspace is split into three invariant Zeno subspaces  $H_{p0} = \{|\psi_1\rangle, |\psi_5\rangle, |\phi_1\rangle\}$ ,  $H_{p1} = \{|\phi_2\rangle\}$ , and  $H_{p2} = \{|\phi_3\rangle\}$ .

The above analysis provides a classical space division via QZD. Nevertheless, it is easily found from Eq. 5 that the transition  $|\psi_1\rangle \leftrightarrow |\phi_2\rangle(|\phi_3\rangle) \leftrightarrow |\psi_5\rangle$  is still difficult to realize even when  $\Omega_k(t)$  is very close to  $\lambda$ . Therefore, we assume  $\sqrt{2}\lambda$  is slightly larger than  $\Omega_k$  and divide the system into three subsystems,

$$S_1 = \{|\psi_1\rangle, |\phi_2\rangle, |\psi_5\rangle\}, S_2 = \{|\psi_1\rangle, |\phi_1\rangle, |\psi_5\rangle\}, S_3 = \{|\psi_1\rangle, |\phi_3\rangle, |\psi_5\rangle\}. \tag{6}$$

We neglect the interaction between the states in each of the subsystems  $S_1$  and  $S_3$  for the moment since the interaction is far weaker than that in subsystem  $S_2$ . Then the system can be considered as a three-level single-atom system with two ground states  $|\psi_1\rangle$  and  $|\psi_5\rangle$  and an excited state  $|\phi_1\rangle$ . If we replace  $|\psi_1\rangle$  as  $|\psi_0\rangle$ , the Hamiltonian for STIRAP reads

$$H_{S_2}(t) = \frac{1}{\sqrt{2}} \begin{pmatrix} 0 & \Omega_1(t) & 0 \\ \Omega_1(t) & 0 & \Omega_2(t) \\ 0 & \Omega_2(t) & 0 \end{pmatrix}. \tag{7}$$

The corresponding instantaneous eigenstates  $|\Phi_n\rangle$ , with eigenvalues  $\eta_0 = 0$  and  $\eta_{\pm} = \pm\chi/\sqrt{2}$ , with  $\chi = \sqrt{\Omega_1^2(t) + \Omega_2^2(t)}$  and  $\theta = \arctan[\Omega_1(t)/\Omega_2(t)]$ , are

$$|\Phi_0(t)\rangle = \begin{pmatrix} \cos \theta \\ 0 \\ -\sin \theta \end{pmatrix}, \quad |\Phi_{\pm}(t)\rangle = \frac{1}{\sqrt{2}} \begin{pmatrix} \sin \theta \\ \pm 1 \\ \cos \theta \end{pmatrix}. \quad (8)$$

Population transfer from the initial state  $|\psi_0\rangle$  to the state  $|\psi_5\rangle$  is achieved adiabatically along the dark state  $|\Phi_0\rangle$  when the adiabatic condition  $|\dot{\theta}| \ll |\frac{1}{\sqrt{2}}\chi|$  is satisfied. To speed up the transfer by using the dynamics of invariant-based inverse engineering, we need to introduce an invariant Hermitian operator  $I_{S_2}(t)$ , which satisfies  $i\partial I_{S_2}(t)/\partial t = [H_{S_2}(t), I_{S_2}(t)]$  [10, 13, 14, 23, 24], for  $H_{S_2}(t)$  possesses the SU(2) dynamical symmetry. And  $I_{S_2}(t)$  is given by

$$I_{S_2}(t) = \frac{1}{\sqrt{2}}\chi \begin{pmatrix} 0 & \cos \gamma \sin \beta & -i \sin \gamma \\ \cos \gamma \sin \beta & 0 & \cos \gamma \cos \beta \\ i \sin \gamma & \cos \gamma \cos \beta & 0 \end{pmatrix}, \quad (9)$$

the time-dependent auxiliary parameters  $\gamma$  and  $\beta$  satisfy the equations

$$\begin{aligned} \dot{\gamma} &= \frac{1}{\sqrt{2}}(\Omega_1 \cos \beta - \Omega_2 \sin \beta), \\ \dot{\beta} &= \frac{1}{\sqrt{2}} \tan \gamma (\Omega_2 \cos \beta + \Omega_1 \sin \beta), \end{aligned} \quad (10)$$

where the dot represents a time derivative. By inversely deriving from eq. (10), the explicit expressions of  $\Omega_1(t)$  and  $\Omega_2(t)$  are as follows:

$$\begin{aligned} \Omega_1(t) &= \sqrt{2}(\dot{\beta} \cot \gamma \sin \beta + \dot{\gamma} \cos \beta), \\ \Omega_2(t) &= \sqrt{2}(\dot{\beta} \cot \gamma \cos \beta - \dot{\gamma} \sin \beta). \end{aligned} \quad (11)$$

The eigenstates  $|\Psi_n\rangle$  of the invariant  $I_{S_2}(t)$ , with eigenvalues  $\varepsilon_0 = 0$  and  $\varepsilon_{\pm} = \pm 1$ , are

$$|\Psi_0(t)\rangle = \begin{pmatrix} \cos \gamma \cos \beta \\ -i \sin \gamma \\ -\cos \gamma \sin \beta \end{pmatrix}, \quad |\Psi_{\pm}(t)\rangle = \frac{1}{\sqrt{2}} \begin{pmatrix} \sin \gamma \cos \beta \pm i \sin \beta \\ i \cos \gamma \\ -\sin \gamma \sin \beta \pm i \cos \beta \end{pmatrix}. \quad (12)$$

The general solution of the Schrödinger equation with respect to the instantaneous eigenstates of  $I_{S_2}(t)$  are written as

$$|\Psi(t)\rangle = \sum_{m=0,\pm} C_m e^{i\alpha_m} |\Psi_m(t)\rangle, \quad (13)$$

where  $C_m$  is a time-independent amplitude and  $\alpha_m$  is the Lewis-Riesenfeld phase according to Lewis Riesenfeld theory [25], and the form of  $\alpha_m$  is

$$\alpha_m(t_f) = \int_0^{t_f} dt \langle \Psi_m(t) | [i \frac{\partial}{\partial t} - H_{S_2}(t)] | \Psi_m(t) \rangle, \quad (14)$$

where  $t_f$  is the total interaction time. Similarly, in our case  $\alpha_0 = 0$ , and

$$\alpha_{\pm} = \mp \int_0^{t_f} dt [\dot{\beta} \sin \gamma + \frac{1}{\sqrt{2}} (\Omega_1 \sin \beta + \Omega_2 \cos \beta) \cos \gamma]. \quad (15)$$

In order to get the target state  $|\psi_5\rangle$  along the invariant eigenstate  $|\Psi_0(t)\rangle$ , we suitably choose the feasible parameters  $\gamma(t)$  and  $\beta(t)$

$$\gamma(t) = \epsilon, \quad \beta(t) = \pi t / 2t_f, \quad (16)$$

where  $\epsilon$  is a small value, which satisfies  $(\sin \epsilon)^{-1} = 4N$  ( $N = 1, 2, 3, \dots$ ) for a high fidelity of the target state [13]. And we obtain

$$\begin{aligned} \Omega_1(t) &= (\pi / \sqrt{2} t_f) \cot \epsilon \sin(\pi t / 2t_f), \\ \Omega_2(t) &= (\pi / \sqrt{2} t_f) \cot \epsilon \cos(\pi t / 2t_f). \end{aligned} \quad (17)$$

Once the Rabi frequencies are specially designed, the FPT of the states in subsystem  $S_2$  will be implemented. Afterwards, we analyze the population transfer of the states in subsystems  $S_1$  and  $S_3$ . Analyzing the population transfer in these two subsystems, by contrast, the whole system must be taken into consideration rather than only the subsystem. We consequently introduce two vectors  $|\mu_1\rangle = \frac{1}{\sqrt{2}}(|\phi_2\rangle - |\phi_3\rangle) = |\psi_3\rangle$  and  $|\mu_2\rangle = \frac{1}{\sqrt{2}}(|\phi_2\rangle + |\phi_3\rangle) = \frac{1}{\sqrt{2}}(|\psi_2\rangle + |\psi_4\rangle)$  for rewriting the Hamiltonian in Eq. (4). We have

$$\begin{aligned} H_{re} &= \frac{1}{\sqrt{2}} \Omega_1(t) (-|\psi_1\rangle \langle \phi_1|) + \frac{1}{\sqrt{2}} \Omega_2(t) |\psi_5\rangle \langle \phi_1| + \frac{1}{\sqrt{2}} \Omega_1(t) |\psi_1\rangle \langle \mu_2| \\ &\quad + \frac{1}{\sqrt{2}} \Omega_2(t) |\psi_5\rangle \langle \mu_2| + \sqrt{2} \lambda |\psi_3\rangle \langle \mu_2| + H.c.. \end{aligned} \quad (18)$$

We find that there is a dark state for the Hamiltonian  $H_{re}$ , and the dark state is

$$\begin{aligned} |Dark\rangle &= \frac{1}{N_2} (\Omega_2(t) |\psi_1\rangle - \frac{\Omega_1(t) \Omega_2(t)}{\lambda} |\psi_3\rangle + \Omega_1(t) |\psi_5\rangle) \\ &= \frac{1}{N_2} [\Omega_2(t) |\psi_1\rangle - \frac{\Omega_1(t) \Omega_2(t)}{\sqrt{2} \lambda} (|\phi_2\rangle - |\phi_3\rangle) + \Omega_1(t) |\psi_5\rangle], \end{aligned} \quad (19)$$

with  $N_2 = \sqrt{\Omega_1^2 + \Omega_2^2 + (\Omega_1 \Omega_2 / \lambda)^2}$ . The result shows that, based on STIRAP, the states  $|\phi_1\rangle$  and  $|\mu_2\rangle$  are neglected when the adiabatic condition for the whole system is satisfied.

However, the adiabatic condition for the whole system can not be satisfied since we have designed two special Rabi frequencies  $\Omega_1$  and  $\Omega_2$ , and we learn from Ref. [13] that the state  $|\phi_1\rangle$  is absolutely populated into a relatively large extent for speeding up the population transfer. Hence, it is very necessary to analyze whether the state  $|\mu_2\rangle$  can still be neglected or not with these two special Rabi frequencies. And the effect of the state  $|\mu_2\rangle$  during the evolution of the whole system is worth studying. By solving the characteristic equation of  $H_{re}$ , we conclude that the smallest difference between an arbitrary eigenvalue and 0 is

$$|\Delta E| = \vartheta/\sqrt{2} = \sqrt{\frac{\Omega_1^2 + \Omega_2^2 + 2\lambda^2 - \varpi}{2}}, \quad (20)$$

with  $\varpi = \sqrt{(\Omega_1^2 - \Omega_2^2)^2 + 4\lambda^4}$  and  $\vartheta = \sqrt{\Omega_1^2 + \Omega_2^2 + 2\lambda^2 - \varpi}$ , the corresponding eigenstates are

$$\begin{aligned} |\Theta_+\rangle &= \frac{1}{N_e} \left\{ \frac{\Omega_1}{\varsigma} \left[ \frac{\vartheta^2}{2} - (\Omega_2^2 + 2\lambda^2) \right] |\psi_1\rangle - \frac{\Omega_2}{\varsigma} \left[ \frac{\vartheta^2}{2} - (\Omega_1^2 + 2\lambda^2) \right] |\psi_5\rangle \right. \\ &\quad \left. - \frac{\vartheta(2\lambda^2 + \varpi)}{2\varsigma} |\phi_1\rangle - \frac{\vartheta}{2\lambda} |\mu_2\rangle + |\psi_3\rangle \right\}, \\ |\Theta_-\rangle &= \frac{1}{N_e} \left\{ \frac{\Omega_1}{\varsigma} \left[ \frac{\vartheta^2}{2} - (\Omega_2^2 + 2\lambda^2) \right] |\psi_1\rangle - \frac{\Omega_2}{\varsigma} \left[ \frac{\vartheta^2}{2} - (\Omega_1^2 + 2\lambda^2) \right] |\psi_5\rangle \right. \\ &\quad \left. + \frac{\vartheta(2\lambda^2 + \varpi)}{2\varsigma} |\phi_1\rangle + \frac{\vartheta}{2\lambda} |\mu_2\rangle + |\psi_3\rangle \right\}, \end{aligned} \quad (21)$$

with  $\varsigma = \lambda(\Omega_1^2 - \Omega_2^2)$ , and  $N_e$  is the corresponding normalization coefficient. Whereas the adiabatic condition for the whole system is not always satisfied, the eigenstates  $|\Theta_+\rangle$  and  $|\Theta_-\rangle$  will be populated and participate in the evolution of the whole system. On account of a wide disparity between the corresponding eigenvalues of the rest eigenstates and 0, these states can be adiabatically eliminated. The states  $|\Theta_+\rangle$  and  $|\Theta_-\rangle$  are similar to each other, thus we take  $|\Theta_+\rangle$  for an example in the following analysis. The ratio  $\tau$  of the coefficients for states  $|\phi_1\rangle$  and  $|\mu_2\rangle$  is

$$\begin{aligned} \tau &= \left| \frac{\vartheta}{\varsigma} \left[ \frac{\vartheta^2}{2} - \left( \frac{\Omega_1^2 + \Omega_2^2}{2} + 2\lambda^2 \right) \right] / \left( -\frac{\vartheta}{2\lambda} \right) \right| \\ &= \left| -\frac{\lambda[\vartheta^2 - (\Omega_1^2 + \Omega_2^2 + 4\lambda^2)]}{\varsigma} \right| \\ &= \left| \frac{2\lambda^2 + \varpi}{\Omega_1^2 - \Omega_2^2} \right|. \end{aligned} \quad (22)$$



If we set  $\Omega_1(t) = \zeta\lambda \sin(\pi/2t_f)$  and  $\Omega_2(t) = \zeta\lambda \cos(\pi/2t_f)$ , where  $\zeta\lambda$  denotes the amplitude of the laser pulse,

$$\tau = \left| \frac{2 + \sqrt{\zeta^4(\sin^2\beta - \cos^2\beta)^2 + 4}}{\zeta^2(\sin^2\beta - \cos^2\beta)} \right|. \quad (23)$$

It is evident, there is a minimum value and a maximum value of  $\tau$ , namely,  $\tau_{min} = |(2 + \sqrt{\zeta^4 + 4})/\zeta^2|$  and  $\tau_{max} = \infty$ . From the conditions described above,  $\zeta < \sqrt{2}$  should be satisfied. When  $\zeta = \sqrt{2}$ ,  $\tau_{min} = 1 + \sqrt{2}$ , and the corresponding ratio of the populations for the states  $|\phi_1\rangle$  and  $|\mu_2\rangle$  is  $\tau^2 = 3 + 2\sqrt{2}$ . The result reveals that, with the limits to the parameters of  $\tau_{min}$ , the population of the state  $|\mu_2\rangle$  is still much less than that of the state  $|\phi_1\rangle$ . And the population of the state  $|\phi_1\rangle$  keeps in a small value during the evolution of the whole system (this will be analyzed in detail later). Afterwards, we deduce that the population for the state  $|\mu_2\rangle$  can be neglected all the time during the evolution. From Eq. (18), we find that the state  $|\psi_3\rangle$  can only be transformed from the state  $|\mu_2\rangle$ . Since the population for the state  $|\mu_2\rangle$  is neglected all the time,  $|\psi_3\rangle$  is considered as an independent state of the whole system. That is, the whole system is regarded as a three-level single-atom system even when the Zeno condition is not well met. However, as the result of strong coupling between the states  $|\mu_2\rangle$  and  $|\psi_3\rangle$ , very little population for the state  $|\mu_2\rangle$  can lead to a rapid increase in the population for the state  $|\psi_3\rangle$ . The effects of the subsystems  $S_1$  and  $S_3$  in the population transfer of the whole system are embodied by the dark state  $|Dark\rangle$ . And the intermediate state  $|\psi_3\rangle$  will become the key point of the combined effect of the subsystems  $S_1$  and  $S_3$  for assisting the population transfer. The population of the intermediate state  $|\psi_3\rangle$  is mainly dominated by the ratio  $r = \Omega_1(t)\Omega_2(t)/(N_2\lambda)$  according to Eq. (21). For simplicity, we set  $t = t_f/2$  (the population of the state  $|\psi_3\rangle$  is the maximum when  $t = t_f/2$ ) such that

$$r = \frac{\pi \cot \epsilon}{\sqrt{(2\sqrt{2}\lambda t_f)^2 + (\pi \cot \epsilon)^2}}, \quad (24)$$

i.e., when  $\epsilon$  is a constant value, the larger the interaction time  $\lambda t_f$  is, the less the population of the intermediate state  $|\psi_3\rangle$  is. From Refs. [10, 13, 17], the essence of FPT in the invariant-based inverse engineering is increasing the populations of some intermediate states under certain conditions. Now, if we suitably increase the population of the intermediate state  $|\psi_3\rangle$  (actually, the population of the state  $|\psi_3\rangle$  is increased by very slightly increasing the population of  $|\mu_2\rangle$ ) with very slightly destroying the conditions for the perfect FPT in the

main subsystem  $S_2$ , the transfer will be much faster for the relation between the population of the state  $|\psi_3\rangle$  and the interaction time is inversely proportional when  $\epsilon$  is a constant value.

The validity of the above theoretical analysis will be numerically proved in the following. First, the population transfer of the whole system is an ideal FPT when the Zeno condition is greatly satisfied. Figure. 2 (a) shows the comparison between the population transfer governed by the total Hamiltonian  $H_I$  according to Eq. (1) and that governed by the Hamiltonian of subsystem  $S_2$  according to Eq. (7) when  $\lambda t_f = 50$  and  $\epsilon = \arcsin 0.25$  [the Zeno condition  $\lambda \gg \Omega_k(t)$  can be satisfied very well], where the markers with different styles and colors represent the time evolution of the populations governed by the subsystem Hamiltonian  $H_{S_2}$  for the states  $|\psi_0\rangle$ ,  $|\psi_5\rangle$ , and  $|\phi_1\rangle$ , respectively, and the curves with different styles and colors represent the time evolution of the populations governed by the total Hamiltonian  $H_I$  for the states  $|\psi_0\rangle$ ,  $|\psi_5\rangle$ ,  $|\phi_1\rangle$ , and  $|\phi_2\rangle$  ( $|\phi_3\rangle$ ), respectively, and the superscripts  $S$  and  $W$  represent the Hamiltonian of the subsystem  $S_2$  and the total Hamiltonian  $H_I$ , respectively. The population for a state  $|\psi\rangle$  is given through the relation  $P = |\langle\psi|\rho(t)|\psi\rangle|$ , where  $\rho(t)$  is the density operator of the system at any time  $t$ . All the time, the populations of the states  $|\phi_2\rangle$  and  $|\phi_3\rangle$  remain negligible, and the time evolution of the system governed by the total Hamiltonian  $H_I$  is exactly the same with the time evolution of the system governed by the subsystem Hamiltonian  $H_{S_2}$  if we neglect the states  $|\phi_2\rangle$  and  $|\phi_3\rangle$ , that is, we quote Chen *et al.* as saying that the whole system evolves along the dark state  $|\Psi_0(t)\rangle$  and an FPT of the whole system can be perfectly achieved. In fact, the dark state  $|\Psi_0(t)\rangle$  can't faultlessly explain the evolution of the system; the system evolves along a special way which is very similar to a dark state, and we name it "dark-like state" for short. This special state has the form  $|D_{like}(t)\rangle = \frac{1}{N_{like}}[\alpha_1(t)|\psi_1\rangle + \alpha_2(t)|\psi_5\rangle + \alpha_3|\phi_1\rangle + \alpha_4(t)|\mu_1\rangle]$ . In the present case, as the Zeno condition is satisfied, the state  $|\mu_1\rangle$  is negligible and the "dark-like state" can be simplified as  $|D'_{like}(t)\rangle = \frac{1}{N'_{like}}[\alpha_1(t)|\psi_1\rangle + \alpha_2(t)|\psi_5\rangle + \alpha_3(t)|\phi_1\rangle]$ .

We confirm that the evolution of the whole system is completely governed by the dark state  $|Dark\rangle$  with completely destroying the conditions for the FPT in the subsystem  $S_2$  [when  $\sin \gamma$  is very close to zero, the invariant Hermitian operator  $I_{S_2}$  according to Eq. (9) equals to the Hamiltonian  $H_{S_2}$ , and the system is just an ordinary system based on STIRAP]. Figure 2 (b) shows the comparison between the population transfer governed by the total Hamiltonian  $H_I$  according to Eq. (1) and that governed by the dark state  $|Dark\rangle$  according to Eq. (19) when  $\lambda t_f = 300$  and  $\epsilon = \arcsin 1/100$  (the condition for STIRAP can

be satisfied), where the markers with different styles and colors represent the time evolution of the populations governed by the dark state  $|Dark\rangle$  for the states  $|\psi_0\rangle$ ,  $|\phi_2\rangle$  ( $|\phi_3\rangle$ ), and  $|\psi_5\rangle$ , respectively, and the curves with different styles and colors represent the time evolution of the populations governed by the total Hamiltonian  $H_I$  for the states  $|\psi_0\rangle$ ,  $|\psi_5\rangle$ ,  $|\phi_1\rangle$ , and  $|\phi_2\rangle$  ( $|\phi_3\rangle$ ), respectively, and superscript  $D$  represents the dark state  $|Dark\rangle$ . Similar to Fig. 2 (a), the time evolution of the whole system is almost absolutely governed by the dark state  $|Dark\rangle$  when the dark state  $|\Psi_0(t)\rangle$  is inoperative for the evolution of the whole system (the conditions for the FPT in the subsystem  $S_2$  are completely ungratified). Contrast Fig. 2 (a) with Fig. 2 (b); the interaction time needed for the FPT in the invariant-based inverse engineering satisfying the Zeno condition is much shorter than the population transfer in an ordinary STIRAP, that is, we have speeded up the population transfer of ground states in a two-atom system with a composed system including the QZD and the invariant-based inverse engineering.

Moreover, we further shorten the interaction time by combining the effect of the subsystem  $S_2$  with the effect of the dark state  $|Dark\rangle$  (the combined effect of the subsystems  $S_1$  and  $S_3$ ). Figure 3 (a) shows the time evolution of the populations governed by the Hamiltonian  $H_{S_2}$  for the states  $|\psi_0\rangle$ ,  $|\phi_1\rangle$ , and  $|\psi_5\rangle$ , Fig. 3 (b) shows the time evolution of the populations governed by the dark state  $|Dark\rangle$  for the states  $|\psi_0\rangle$ ,  $|\phi_2\rangle$  ( $|\phi_3\rangle$ ), and  $|\psi_5\rangle$ , and Fig. 3 (c) shows the time evolution of the populations governed by the total Hamiltonian  $H_I$  for the states  $|\psi_0\rangle$ ,  $|\phi_1\rangle$ ,  $|\phi_2\rangle$  ( $|\phi_3\rangle$ ), and  $|\psi_5\rangle$ . Figs. 3(a)-3(c) are plotted with  $\epsilon = \arcsin 0.25$  ( $N = 1$ ) and  $\lambda t_f = 10$ . Contrast Fig. 3 (c) with Figs. 3 (a) and 3 (b); the time evolution of the whole system governed by the combined effect of the subsystem  $S_2$  and the dark state  $|Dark\rangle$  is a little more complex than that governed by the effect of directly adding these two effects together. It can be seen from Fig. 3 (c) that the population of the target state  $|\psi_5\rangle$  is only 99.35% when  $t = t_f$ . The reason for these results can be understood by the conditions (the Zeno condition, the condition for STIRAP, etc.) for whether an ideal FPT governed by the subsystem  $S_2$  or an ideal population transfer governed by the dark state  $|Dark\rangle$  can not be satisfied very well, actually the population transfer from the initial state to the target state along a dark-like state  $|Dark\rangle_{like}$  which will be discussed in detail elsewhere. Due to the slightly populated intermediate state  $|\mu_2\rangle$ , the whole system can not be faultlessly considered as a three-level single-atom system, and the optimal value of  $\epsilon$  for the whole system will not faultlessly satisfy the condition  $(\sin \epsilon)^{-1} = 4N$  ( $N = 1, 2, 3, \dots$ ). Reselecting the

optimal value of  $\epsilon$  becomes a necessity. We plot the fidelity  $F$  of the target state  $|\psi_5\rangle$  versus the value of  $\epsilon$  and the interaction time  $\lambda t_f$  in FIG. 3 (d). The fidelity  $F$  for the target state  $|\psi_5\rangle$  is given through the relation  $F = |\langle\psi_5|\rho(t_f)|\psi_5\rangle|$ , where  $\rho(t_f)$  is the density operator of the system at the time  $t_f$  by solving the differential equation  $\dot{\rho} = i[\rho, H_I]$ . When  $\lambda t_f = 10$ , the optimal value of  $\epsilon$  for the highest fidelity ( $F = 1$ ) of the state  $|\psi_5\rangle$  is about 0.2636, meanwhile, the minimum value of  $\lambda t_f$  is only about 7.3 for a perfect FPT ( $F = 1$  for the target state when  $t = t_f$ ), even when  $\lambda t_f = 6.4$  and  $\epsilon \approx 0.26$ , the fidelity of the target state is higher than 99% (when  $\lambda t_f < 6$ , the whole system can not be considered as a three-level single-atom system since the state  $|\mu_2\rangle$  is populated too much and can not be neglected). What is more, this method is insensitive to the fluctuations of  $\epsilon$  and the interaction time  $\lambda t_f$ , and is also insensitive to the amplitude of the laser pulses and the coupling constant  $\lambda$ . For convenient discussion, we suitably choose three sets of parameters  $\{\epsilon = 0.2636, \lambda t_f = 10\}$ ,  $\{\epsilon = 0.1196, \lambda t_f = 20\}$ , and  $\{\epsilon = 0.0810, \lambda t_f = 40\}$ , corresponding  $N = 1$ ,  $N = 2$ , and  $N = 3$ , respectively. Figure 4 (a) shows the time dependence of the Rabi frequencies for the atoms when  $\epsilon = 0.2636$  and  $\lambda t_f = 10$ . The ratio  $\Omega_k^{max}/\lambda$  (here the superscript *max* denotes the maximum value of  $\Omega_k$ ) is 0.8232 which meets the conditions mentioned above. And Fig. 4 (b) shows the time evolution of the populations for states  $|\psi_0\rangle$ ,  $|\psi_2\rangle$ ,  $|\psi_3\rangle$ ,  $|\psi_4\rangle$ , and  $|\psi_5\rangle$ . After reselecting the optimal value of  $\epsilon$ , a perfect population transfer from the initial state  $|\psi_0\rangle$  to the target state  $|\psi_5\rangle$  (the population of the target state  $|\psi_5\rangle$  is 1 when  $t = t_f$ ) can be achieved. Figure 5 (a) shows the time evolution of the populations for the states  $|\phi_1\rangle$  ( $|\mu_1\rangle$ ),  $|\psi_3\rangle$ , and  $|\mu_2\rangle$ . The population of  $|\mu_2\rangle$  remain negligible all the time even with  $\zeta = 0.8232$ . Actually, Fig. 5 (a) explains the essence of FPT. The intermediate states  $|\phi_1\rangle$ ,  $|\psi_3\rangle$ , and  $|\mu_2\rangle$  are usually neglected in the schemes in the view of STIRAP and QZD. However, these states are necessary for the transfer from the initial state  $|\psi_0\rangle$  to the target state  $|\psi_5\rangle$ . They link the whole system together just like brittle strings; the evolution of the system is interdictory without the participation of these intermediate states. By increasing the populations of intermediate states in a certain period of time, just like broadening the channels for the transition between  $|\psi_0\rangle \leftrightarrow |\psi_5\rangle$  in a certain period of time, the transition could be much faster. Figures. 4 and 5 (a) are plotted when  $\lambda t_f = 10$  and  $\epsilon = 0.2636$ . Figure 5 (b) shows the populations for the states  $|\psi_0\rangle$ ,  $|\psi_2\rangle$ ,  $|\psi_3\rangle$ ,  $|\psi_4\rangle$ , and  $|\psi_5\rangle$  when  $\lambda t_f = 20$  and  $\epsilon = 0.1196$ . Contrast Fig. 4 (b) with Fig. 5 (b); it turns out that a longer interaction time is required, i.e.,  $t_f = 20/\lambda$ , when  $\epsilon = 0.1196$  for achieving the target state, and the

population of  $|\psi_3\rangle$  only changes a little while the populations of  $|\psi_2\rangle$  and  $|\psi_4\rangle$  change a lot. The reason for needing a longer interaction time is that a smaller  $\epsilon$  causes larger amplitudes of the laser pulses, and a relatively larger  $\lambda t_f$  should be chosen to satisfy the conditions above. As narrated above, the population of  $|\psi_3\rangle$  is only governed by the combined effect of subsystems  $S_1$  and  $S_3$ . The ratio  $r$  governs the population of the state  $|\psi_3\rangle$  according to eq. (24). We obviously have to have the ratio  $r = 0.4195$  when  $\lambda t_f = 20$  and  $\epsilon = 0.1196$ , and  $r = 0.3806$  when  $\lambda t_f = 10$  and  $\epsilon = 0.2636$ . This immediately implies, by varying  $\lambda t_f$  and  $\epsilon$  at a similar rate, the corresponding ratio  $r$  shifts only a little bit. That is the reason why the population of  $|\psi_3\rangle$  almost keeps unchanging when  $\lambda t_f$  and  $\cot \epsilon$  are changing similarly.

In particular, we contrast this method with an ordinary method based on QZD with the similar model. When the Zeno condition  $\lambda \gg \Omega_k$  is satisfied and the laser pulses are independent of time, based on the QZD, an effective Hamiltonian of the system is

$$H_{eff} = \frac{\Omega_1}{\sqrt{2}}|\psi_0\rangle\langle\phi_1| + \frac{\Omega_2}{\sqrt{2}}|\psi_5\rangle\langle\phi_1| + H.c., \quad (25)$$

and the general evolution form of eq. (25) at time  $t$  is

$$|\psi(t)\rangle = \frac{1}{2\chi^2}(\Omega_1^2 \cos \chi t + \Omega_2^2)|\psi_0\rangle - i \sin \chi t |\phi_1\rangle + \frac{1}{2\chi^2}(\Omega_1\Omega_2 \cos \chi t - \Omega_1\Omega_2)|\psi_5\rangle, \quad (26)$$

with  $\chi = \sqrt{(\Omega_1^2 + \Omega_2^2)/2}$ . When we choose  $t = t_f = \pi/\chi$  and  $\Omega_Z = \Omega_1 = \Omega_2$ , the target state  $|\psi_5\rangle$  is obtained. For  $\lambda t_f = \pi/\Omega_Z$ , if  $\Omega_Z = 0.1\lambda$  (almost the limitation of the value of  $\Omega_Z$  for satisfying the Zeno condition),  $t_f \simeq 31.416\lambda$ . The maximal population of the intermediate  $|\phi_1\rangle$  during the evolution of the whole system is 50% when  $t = 0.5t_f$ , that means the influence of decoherence caused by the spontaneous emission is very great. The minimum effective interaction time  $\lambda t_f$  as mentioned above, however, is only about 7.2. As noted earlier, the QZD is sensitive to variations in some parameters, especially the interaction time. Whereas, this method is insensitive to variations in most of the parameters. Compare to the method based on STRIRAP and QZD, this method has superiority to some extent.

In the above discussion, the dissipation has not been taken into account. However, the system will interact with the environment inevitably which effects the availability of this method. Thus, we investigate the influence of spontaneous emission and photon leakage on this method. Once considered, the evolution of the system can be modeled by a master equation in Lindblad form

$$\dot{\rho} = i[\rho, H_{tot}] + \sum_k [L_k \rho L_k^\dagger - \frac{1}{2}(L_k^\dagger L_k \rho + \rho L_k^\dagger L_k)], \quad (27)$$

where the  $L_k$ 's are the so-called Lindblad operators [26]. The five Lindblad operators governing dissipation in the two-atom model are

$$L_1^\kappa = \sqrt{\kappa}a, \quad L_2^\Gamma = \sqrt{\Gamma_1}|f\rangle_1\langle e|, \quad L_3^\Gamma = \sqrt{\Gamma_2}|f\rangle_2\langle e|, \quad L_4^\Gamma = \sqrt{\Gamma_3}|g\rangle_1\langle e|, \quad L_5^\Gamma = \sqrt{\Gamma_4}|g\rangle_2\langle e|, \quad (28)$$

where  $\kappa$  is the decay of the cavity and  $\Gamma_i$  ( $i = 1, 2, 3, 4$ ) are the spontaneous emissions of atoms. Without loss of generality, we set  $\Gamma_i = \Gamma/2$ . The fidelity  $F$  for the target state  $|\psi_5\rangle$  is given through the relation  $F = |\langle\psi_5|\rho(t_f)|\psi_5\rangle|$ , where  $\rho(t_f)$  is the density operator of the system at the time  $t_f$ . In Fig. 6 (a) we plot the fidelity  $F$  of the target state  $|\psi_5\rangle$  versus the decay of spontaneous emission  $\Gamma/\lambda$  with different values of  $\epsilon$  and  $\lambda t_f$  when the decay of cavity  $\kappa/\lambda = 0$ . The result shows that the larger the value of  $\epsilon$  is, the more sensitive to the decay of spontaneous emission the system is. The reason for this result is that the populations of effective intermediate states  $|\psi_2\rangle$  and  $|\psi_4\rangle$  decrease as  $\epsilon$  gets smaller. Figure 6 (b) shows the fidelity  $F$  of the target state  $|\psi_5\rangle$  versus the decay of cavity  $\kappa/\lambda$  with different values of  $\epsilon$  and  $\lambda t_f$  when the decay of spontaneous emission  $\Gamma/\lambda = 0$ . The sensitivity of the system to the decay of cavity seemingly decreases with the decreasing of  $\epsilon$ . Because the population of the effective intermediate state  $|\psi_3\rangle$  is mainly dominated by the ratio  $r$ , and the Zeno condition ( $\lambda \gg \Omega_k$ ) could be satisfied very well when the ratio  $r$  is small enough, that is, the intermediate state  $|\psi_3\rangle$  can be effectively neglected with an adequately small ratio  $r$ . Thus  $r = 0.3806$  when  $\epsilon = 0.2636$  and  $\lambda t_f = 10$ ,  $r = 0.4195$  when  $\epsilon = 0.1196$  and  $\lambda t_f = 20$ , and  $r = 0.3273$  when  $\epsilon = 0.0810$  and  $\lambda t_f = 40$ . The population of  $|\psi_3\rangle$  is the smallest when  $\epsilon = 0.0810$  for the three sets of parameters in Fig. 6. As it is known, the interaction time  $\lambda t_f$  also governs the decoherence of the system. Considering both the population of the state  $|\psi_3\rangle$  and the interaction time, the most insensitive to the decay of cavity is at  $\epsilon = 0.2636$  and  $\lambda t_f = 10$ . Contrast Fig. 6 (a) with Fig. 6 (b); an increase in the decay rate  $\kappa$  reduces the stationary state fidelity more rapidly than an increase in the decay rate  $\Gamma$ .

The relationship of the fidelity  $F$  of the target state  $|\psi_5\rangle$  versus the ratios  $\kappa/\lambda$  and  $\Gamma/\lambda$  by solving the master equation numerically is shown in Fig. 7 (a) when  $\epsilon = 0.2636$  and  $\lambda t_f = 10$ . The fidelity  $F$  decreases slowly with the increasing of cavity decay and atomic spontaneous emission and it is robust against to cavity decay and atomic spontaneous emission since it is still about 87.03% when  $\kappa/\lambda = \Gamma/\lambda = 0.1$ . Therefore, our scheme is robust against the two error sources and could acquire a better result in realistic conditions.

### III. FAST POPULATIONS TRANSFER IN THE MULTIPARTICLE SYSTEMS

Actually, this method can be effectively applied to a multiparticle system for achieving the FPTs, generating entangled states, implementing phase gates, etc.. Assume that all of the atoms are trapped in one cavity, in the interaction picture, the Hamiltonian of a cavity-atom combined system can be described as

$$H_i = H_{ac} + H_{al} + H_{aa}, \quad (29)$$

where  $H_{ac}$  is the Hamiltonian for the interaction between the atoms and the cavity,  $H_{al}$  is the Hamiltonian for the interaction between the atoms and the time-dependent laser pulses, and  $H_{aa}$  is the Hamiltonian for the direct interaction between the atoms. In a typical setup with neutral atoms at least several microns apart direct interactions are negligible,  $H_{aa} = 0$ . Just as QZD, with the eigenvectors of  $H_{ac}$ , we rewrite the Hamiltonian  $H_{al}$  and  $H_{ac}$  as  $H'_{al}$  and  $H'_{ac}$ , respectively. By solving the characteristic equation of  $H_{ac}$ , a set of eigenvalues  $\xi_n = \sum C_{n,m} \lambda_m$  is gained. Here  $\lambda_m$  is the  $m$ th coupling constant between the atoms and cavity. Setting  $\lambda_m = \lambda$  for simplicity, we get a set of eigenvalues  $\xi_n = C'_n \lambda$ . The Hamiltonian are given by

$$\begin{aligned} H_i &= H'_{ac} + H'_{al}, \\ H'_{ac} &= \sum_n \xi_n |\Phi_n\rangle \langle \Phi_n|, \\ H'_{al} &= \sum_{n,m,l} b_{n,m,l} \Omega_m(t) |\Phi_n\rangle \langle \varphi_l| + H.c., \end{aligned} \quad (30)$$

where  $|\Phi_n\rangle$  is the  $n$ th eigenvector for the Hamiltonian  $H_{ac}$ ,  $\Omega_m(t)$  is the  $m$ th Rabi frequency for the whole system,  $|\varphi_l\rangle$  is the  $l$ th basis vector for the whole system, and  $b_{n,m,l}$  is the corresponding  $\{n, m, l\}$ th coefficient. Almost the same as the transition between Eq. (4) and Eq. (5), we perform a unitary transformation  $U = e^{-iH'_{ac}t}$  on  $H'_{al}$  under the condition  $H'_{al} \ll H'_{ac}$ . We find that the Hamiltonian becomes  $H_{al}^{eff}$ ,

$$H_{al}^{eff} = \sum_{n,m,l} b_{n,m,l} \Omega_m(t) e^{i\xi_n t} |\Phi_n\rangle \langle \varphi_l| + H.c.. \quad (31)$$

Suppose that there are  $M$  different eigenvalues for the Hamiltonian  $H_{ac}$ , and the corresponding eigenvalues are  $0, \pm\lambda, \pm\sqrt{2}\lambda, \pm\sqrt{3}\lambda, \dots$ . By utilizing the analysis in section II, we

consider the terms with  $\xi_n = 0$  as the main subsystem  $S_1$  for the whole system, and the terms with eigenvalues  $\pm\lambda$  as the secondary subsystems  $S_2^+$  and  $S_2^-$ , and so on. Firstly, we design, by invariant-based inverse engineering, resonant laser pulses to perform a FPT in the main subsystem  $S_1$ . Secondly, by setting some simple conditions, a part of the subsystems can be neglected since the interaction between the states in each of these subsystems is far weaker than that in the main subsystem. Introducing some special vectors (a part of these vectors can be neglected all the time during the evolution of the whole system and the rest of the vectors only have direct interaction with the vectors which are neglected), we rewrite the total Hamiltonian and find out the dark state.

Next, the most important work is how to design and perform the FPT in the subsystem  $S_1$ . From refs [10, 13, 17], we know that it is very hard to directly design and perform the FPT in a system which is more complicated than the three-level single-atom system. It is best to perform an equivalent transformation to make the subsystem  $S_1$  become a system which can be considered as a two-level or three-level single-atom system. And the part of these operations for achieving the “excited state” of the “two-level or three-level single-atom system” can be finished based on the superposition principle and Gram-Schmidt orthonormalization since all of the states  $|\Phi_n\rangle$  in this subsystem have the same eigenvalue  $\xi = 0$ . We cipher out the conditions for neglecting the special vectors. The whole system is alike to the two-atom system mentioned in Sec. II, and then the FPT in a multiparticle system can be effectively achieved.

We now consider three atoms are trapped in a bimodal-mode cavity. Each atom has one excited state  $|e\rangle$  and three ground states  $|f\rangle$ ,  $|g_+\rangle$ , and  $|g_-\rangle$ . The transition  $|f\rangle \leftrightarrow |e\rangle$  is resonantly driven through a time-dependent laser pulse with Rabi frequency  $\Omega(t)$ , and the transition  $|g_+\rangle(|g_-\rangle) \leftrightarrow |e\rangle$  is resonantly coupled to the left-circularly (right-circularly) polarized cavity mode with coupling constant  $\lambda_+(\lambda_-)$ . The transition  $|g_+\rangle_1(|g_-\rangle_3) \leftrightarrow |e\rangle$  and  $|f\rangle \leftrightarrow |e\rangle$  is supposed to be closed for atom  $a_1(a_3)$  and atom  $a_2$ , respectively. As a consequence, the total Hamiltonian in the interaction picture is given by

$$H_I = H_{al} + H_{ac},$$

$$H_{al} = \sum_{k=1,3} \Omega_k(t) |e\rangle_k \langle f| + H.c.,$$



$$H_{ac} = \lambda_{1,+}|e\rangle_1\langle g_+|a_+ + \lambda_{2,+}|e\rangle_2\langle g_+|a_+ + \lambda_{2,-}|e\rangle_2\langle g_-|a_- + \lambda_{3,-}|e\rangle_3\langle g_-|a_- + H.c., \quad (32)$$

where the subscripts 1, 2, and 3 represent the atoms  $a_1$ ,  $a_2$ , and  $a_3$ , respectively.  $a_{\pm}$  are the annihilation operators for the cavity modes. We assume the initial state is  $|f\rangle_1|g_+\rangle_2|g_-\rangle_3|0\rangle_c$  and  $\lambda_{k,\pm} = \lambda$  ( $k = 1, 2, 3$ ). The basis vectors for the whole system are

$$\begin{aligned} |\varphi_1\rangle &= |f\rangle_1|g_+\rangle_2|g_-\rangle_3|0\rangle_c, \\ |\varphi_2\rangle &= |e\rangle_1|g_+\rangle_2|g_-\rangle_3|0\rangle_c, \\ |\varphi_3\rangle &= |g_+\rangle_1|g_+\rangle_2|g_-\rangle_3|1\rangle_c, \\ |\varphi_4\rangle &= |g_+\rangle_1|e\rangle_2|g_-\rangle_3|0\rangle_c, \\ |\varphi_5\rangle &= |g_+\rangle_1|g_-\rangle_2|g_-\rangle_3|1\rangle_c, \\ |\varphi_6\rangle &= |g_+\rangle_1|g_-\rangle_2|e\rangle_3|0\rangle_c, \\ |\varphi_7\rangle &= |g_+\rangle_1|g_-\rangle_2|f\rangle_3|0\rangle_c, \end{aligned} \quad (33)$$

and the eigenvectors for the Hamiltonian  $H_{ac}$  are

$$\begin{aligned} |\Phi_1\rangle &= \frac{1}{\sqrt{3}}(|\varphi_2\rangle - |\varphi_4\rangle + |\varphi_6\rangle), \\ |\Phi_2\rangle &= \frac{1}{2}(-|\varphi_2\rangle - |\varphi_3\rangle + |\varphi_5\rangle + |\varphi_6\rangle), \\ |\Phi_3\rangle &= \frac{1}{2}(-|\varphi_2\rangle + |\varphi_3\rangle - |\varphi_5\rangle + |\varphi_6\rangle), \\ |\Phi_4\rangle &= \frac{1}{2\sqrt{2}}(|\varphi_2\rangle + \sqrt{3}|\varphi_3\rangle + 2|\varphi_4\rangle + \sqrt{3}|\varphi_5\rangle + |\varphi_6\rangle), \\ |\Phi_5\rangle &= \frac{1}{2\sqrt{2}}(|\varphi_2\rangle - \sqrt{3}|\varphi_3\rangle + 2|\varphi_4\rangle - \sqrt{3}|\varphi_5\rangle + |\varphi_6\rangle), \end{aligned} \quad (34)$$

with eigenvalues  $\xi_1 = 0$ ,  $\xi_2 = \lambda$ ,  $\xi_3 = -\lambda$ ,  $\xi_4 = \sqrt{3}\lambda$ , and  $\xi_5 = -\sqrt{3}\lambda$ . It is verified that the  $H_{al}^{eff}$  is

$$\begin{aligned} H_{al}^{eff} &= \frac{1}{\sqrt{3}}|\Phi_1\rangle(\Omega_1(t)\langle\varphi_1| + \Omega_3(t)\langle\varphi_7|) \\ &\quad + \frac{1}{2}|\Phi_2\rangle(-\Omega_1(t)\langle\varphi_1| + \Omega_3(t)\langle\varphi_7|)e^{i\lambda t} \\ &\quad + \frac{1}{2}|\Phi_3\rangle(-\Omega_1(t)\langle\varphi_1| + \Omega_3(t)\langle\varphi_7|)e^{-i\lambda t} \\ &\quad + \frac{1}{2\sqrt{3}}|\Phi_4\rangle(\Omega_1(t)\langle\varphi_1| + \Omega_3(t)\langle\varphi_7|)e^{i\sqrt{3}\lambda t} \\ &\quad + \frac{1}{2\sqrt{3}}|\Phi_5\rangle(\Omega_1(t)\langle\varphi_1| + \Omega_3(t)\langle\varphi_7|)e^{-i\sqrt{3}\lambda t} + H.c.. \end{aligned} \quad (35)$$

Caused by five different eigenvalues of the Hamiltonian  $H_{ac}$ , we divide the system into five subsystems,

$$S_1 = \{|\varphi_1\rangle, |\Phi_1\rangle, |\varphi_7\rangle\}, S_2^+ = \{|\varphi_1\rangle, |\Phi_2\rangle, |\varphi_7\rangle\}, S_2^- = \{|\varphi_1\rangle, |\Phi_3\rangle, |\varphi_7\rangle\},$$

$$S_3^+ = \{|\varphi_1\rangle, |\Phi_4\rangle, |\varphi_7\rangle\}, S_3^- = \{|\varphi_1\rangle, |\Phi_5\rangle, |\varphi_7\rangle\}. \quad (36)$$

The main subsystem  $S_1$  can be considered as a three-level single-atom system. If we set “ $\sqrt{2}\lambda$  is slightly larger than  $\Omega_k$ ” (actually, the setting varies depending on the method), the terms containing the oscillating frequency  $\pm\sqrt{3}\lambda$  will be effectively neglected, that is, the subsystems  $S_3^\pm$  can be effectively neglected. The two vectors introduced for rewriting the total Hamiltonian in eq. (32) are  $|\mu_+\rangle = \frac{1}{\sqrt{2}}(|\Phi_2\rangle - |\Phi_3\rangle)$  and  $|\mu_-\rangle = \frac{1}{\sqrt{2}}(|\Phi_2\rangle + |\Phi_3\rangle)$ . The whole system evolves in the subspace spanned by the basis vectors  $\{|\varphi_1\rangle, |\varphi_7\rangle, |\Phi_1\rangle, |\mu_+\rangle, |\mu_-\rangle\}$ . In terms of the basis vectors, the total Hermitian in the interaction picture is simplified as

$$H_{re}^3 = \frac{1}{\sqrt{3}}|\Phi_1\rangle(\Omega_1(t)\langle\varphi_1| + \Omega_3(t)\langle\varphi_7|) + \frac{1}{\sqrt{2}}|\mu_-\rangle(-\Omega_1(t)\langle\varphi_1| + \Omega_3(t)\langle\varphi_7|) + \lambda|\mu_-\rangle\langle\mu_+| + H.c.. \quad (37)$$

An ideal FPT is performed effectively in the whole system, and it is the same as what we have done in section II. First, we design the two special Rabi frequencies by using the dynamics of invariant-based inverse engineering. The Hermitian  $H_{S_1}^3$  for the main subsystem  $S_1$  of the three-atom model reads

$$H_{S_1}^3(t) = \frac{1}{\sqrt{3}} \begin{pmatrix} 0 & \Omega_1(t) & 0 \\ \Omega_1(t) & 0 & \Omega_3(t) \\ 0 & \Omega_3(t) & 0 \end{pmatrix}. \quad (38)$$

And the corresponding invariant Hermitian operator  $I_{S_1}^3(t)$  satisfying  $i\partial I_{S_1}^3(t)/\partial t = [H_{S_1}^3(t), I_{S_1}^3(t)]$  for speeding up the transfer is

$$I_{S_1}^3(t) = \frac{1}{\sqrt{3}}\chi' \begin{pmatrix} 0 & \cos\gamma' \sin\beta' & -i \sin\gamma' \\ \cos\gamma' \sin\beta' & 0 & \cos\gamma' \cos\beta' \\ i \sin\gamma' & \cos\gamma' \cos\beta' & 0 \end{pmatrix}, \quad (39)$$

where  $\chi'$  is an arbitrary constant with units of frequency to keep  $I_{S_1}^3(t)$  involving the energy dimension. Then the two special Rabi frequencies designed for performing the FPT in the main subsystem  $S_1$  are inferred,

$$\begin{aligned} \Omega_1(t) &= \sqrt{3}(\dot{\beta}' \cot\gamma' \sin\beta' + \dot{\gamma}' \cos\beta'), \\ \Omega_3(t) &= \sqrt{3}(\dot{\beta}' \cot\gamma' \cos\beta' - \dot{\gamma}' \sin\beta'). \end{aligned} \quad (40)$$

We also choose  $\gamma' = \epsilon$  and  $\beta' = \pi t/t_f$ , where  $\epsilon$  is also a small value which should be carefully chosen later for a high fidelity of the transfer. Substituting  $\gamma'$  and  $\beta'$  into eq.(40), the two special Rabi frequencies turnout to be

$$\begin{aligned}\Omega_1(t) &= (\sqrt{3}\pi/2t_f) \cot \epsilon \sin(\pi t/2t_f), \\ \Omega_3(t) &= (\sqrt{3}\pi/2t_f) \cot \epsilon \cos(\pi t/2t_f).\end{aligned}\quad (41)$$

Second, we make the secondary subsystems  $S_2^\pm$  become the auxiliary for the FPT in the whole system. By solving the intrinsic equation of  $H_{re}^3$ , the dark state for the whole system is obtained,

$$\begin{aligned}|Dark_3\rangle &= \frac{1}{\sqrt{N_3}}[\Omega_3(t)|\varphi_1\rangle - \frac{\Omega_1(t)\Omega_3(t)}{\lambda}(|\varphi_3\rangle - |\varphi_5\rangle) - \Omega_1(t)|\varphi_7\rangle] \\ &= \frac{1}{\sqrt{N_3}}[\Omega_3(t)|\varphi_1\rangle + \frac{\Omega_1(t)\Omega_3(t)}{\lambda}(|\Phi_2\rangle - |\Phi_3\rangle) - \Omega_1(t)|\varphi_7\rangle], \\ &= \frac{1}{\sqrt{N_3}}[\Omega_3(t)|\varphi_1\rangle + \frac{\sqrt{2}\Omega_1(t)\Omega_3(t)}{\lambda}|\mu_+\rangle - \Omega_1(t)|\varphi_7\rangle],\end{aligned}\quad (42)$$

with  $N_3 = \sqrt{\Omega_1(t)^2 + \Omega_3(t)^2 + 2(\Omega_1(t)\Omega_3(t)/\lambda)^2}$ . The intermediate state  $|\mu_-\rangle$  is considered as a state which can be neglected all the time and the state  $|\mu_+\rangle$  is considered as an independent state of the system under certain conditions. By setting the condition for very slightly increasing the population of  $|\mu_-\rangle$ , the FPT of the whole system can be achieved. And a very short interaction time i.e.,  $\lambda t_f = 9.5$ , is needed for achieving a perfect target state  $|\varphi_7\rangle$  with a fidelity 99.9% from the initial state  $|\varphi_1\rangle$  when  $\epsilon = 0.2596$  by the numerical calculation. Figure 8 (a) shows the time evolution of the populations for states  $|\varphi_1\rangle - |\varphi_7\rangle$ . Figure 8 (b) is plotted to demonstrate that the subsystems  $S_3^\pm$  and the state  $|\mu_-\rangle$  can be effectively neglected. From Fig. 8 (b), it is displayed that the populations of the states  $|\Phi_4\rangle$  and  $|\Phi_5\rangle$  remain negligible all the time since the maximum values of the populations are only 0.82% for the states  $|\Phi_4\rangle$  and  $|\Phi_5\rangle$ . The state  $|\mu_-\rangle$  is very slightly populated for speeding up the population transfer, and it still can be considered as negligible since the maximum value of its population is only 4.8%. Figs. 8 (a) and (b) are plotted when  $\epsilon = 0.2596$  and  $\lambda t_f = 9.5$ . The fidelity of the target state  $|\varphi_7\rangle$  in the presence of decoherence is given through solving the master equation according to Eq. (27). There are eight Lindblad operators for the three-atom model,

$$L_1^\kappa = \sqrt{\kappa_+}a_+, \quad L_2^\kappa = \sqrt{\kappa_-}a_-, \quad L_3^\Gamma = \sqrt{\Gamma_1}|f\rangle_1\langle e|, \quad L_4^\Gamma = \sqrt{\Gamma_2}|f\rangle_3\langle e|,$$

$$L_5^\Gamma = \sqrt{\Gamma_3}|g_+\rangle_1\langle e|, L_6^\Gamma = \sqrt{\Gamma_4}|g_-\rangle_3\langle e|, L_7^\Gamma = \sqrt{\Gamma_5}|g_+\rangle_2\langle e|, L_8^\Gamma = \sqrt{\Gamma_6}|g_-\rangle_2\langle e|. \quad (43)$$

We also set  $\kappa_i = \kappa$  ( $i = +, -$ ) and  $\Gamma_j = \Gamma/2$  ( $j = 1, 2, \dots, 6$ ) for simplicity. From the relationship of fidelity  $F$  of the target state  $|\varphi_7\rangle$  versus the ratios  $\kappa/\lambda$  and  $\Gamma/\lambda$  given in FIG. 7 (b),  $F$  decreases slowly with the increasing of cavity decay and atomic spontaneous emission and it is insensitive to both of these two error sources because it is still about 88.89% when  $\kappa = \Gamma = 0.05\lambda$ .

#### IV. CONCLUSION

The invariant-based inverse method presented here may be compared to the optimal control approaches in Refs. [13, 27–29], it provides a complementary perspective of these approaches, whereas optimal control is useful to choose among the possible solutions found by the invariant-based inverse engineering [13]. The QZD is a very effective method and it has been widely used in quantum information processing [30–33]. It is well known that the QZD has the advantage of simplifying a complicated system by space division, and the shortcuts to adiabatic passage mentioned by Chen *et al.* has the advantage of shortening the operation time by using special resonant pulses. In this paper, we combine the advantage of “simplifying a complicated system” with the advantage of “shortening the operation time”, and present a method for performing the FPTs in multiparticle systems. Two different models have been discussed, and a perfect target state can be achieved in a very short interaction time in each of the two models. But some relatively large laser intensities are needed since shortening the time implies an energy cost [13]. In a more general case, if there are no eigenvalues  $\xi_n = 0$  for the Hamiltonian  $H_{ac}$ , the Hamiltonian for the main subsystem  $H_{S_1}$  does not possess SU(2) symmetry, so that the invariant  $I_{S_1}$  should be constructed in terms of the eight Gell-Mann matrices for the SU(3) group [34].

In experiment, the atom cesium can be used for this method. And a set of cavity QED parameters  $(\lambda, \kappa, \Gamma)/2\pi = (750, 3.5, 2.62)$  MHz is predicted to be available in an optical cavity [35], therefore, the fidelity for the target state is still higher than 99.2% for the two-atom system. With these parameters, it allows us to construct an atomic system for the FPT in the presence of decoherence.

In summary, we have proposed a promising method to construct shortcuts to perform the FPT for ground states in two or more atoms systems by invariant-based inverse engineering

and in the view of quantum Zeno dynamics in the cavity QED system. Compared with the previous works, the present work can perform perfect FPTs in multiparticle systems without additional complex conditions. And this method is insensitive to the variations of the parameters, at the same time, the interaction time needs not to be controlled accurately. We firmly believe that this work will make contributions to quantum information processing including performing atomic transport, implementing quantum gates, generating entangled states, etc..

## V. ACKNOWLEDGMENTS

This work was supported by the National Natural Science Foundation of China under Grants No. 11205037 and No. 11105030, the Major State Basic Research Development Program of China under Grant No. 2012CB921601,

- 
- [1] J. Lee, M. Paternostro, M. S. Kim, and S. Bose, Phys. Rev. Lett. **96**, 080501 (2006).
  - [2] K. Bergmann, H. Theuer, and B. W. Shore, Rev. Mod. Phys. **70**, 1003 (1998).
  - [3] P. Král, I. Thanopoulos, and M. Shapiro, Rev. Mod. Phys. **79**, 53 (2007).
  - [4] N. V. Vitanov, T. Halfmann, B. W. Shore, and K. Bergmann, Annu. Rev. Phys. Chem. **52**, 763 (2001).
  - [5] C. P. Yang, Phys. Rev. A **82**, 054303 (2010).
  - [6] M. Amnat-Talab, S. Guérin, N. Sangouard, and H. R. Jauslin, Phys. Rev. A **71**, 023805 (2005).
  - [7] A. Ruschhaupt, X. Chen, D. Alonso, and J. G. Muga, New J. Phys. **14**, 093040 (2012).
  - [8] M. Demirplak and S. A. Rice, J. Phys. Chem. A **107**, 9937 (2003).
  - [9] M. Demirplak and S. A. Rice, J. Chem. Phys. **129**, 154111 (2008).
  - [10] X. Chen, I. Lizuain, A. Ruschhaupt, D. Guéry-Odelin, and J. G. Muga, Phys. Rev. Lett. **105**, 123003 (2010).
  - [11] S. Masuda and K. Nakamura, Proc. R. Soc. Lond. A **466**, 1135 (2010).
  - [12] M. B. Berry, J. Phys. A: Math. Theor. **42**, 365303 (2009).
  - [13] X. Chen and J. G. Muga, Phys. Rev. A **86**, 033405 (2012).

- [14] X. Chen, E. Torrontegui, and J. G. Muga, Phys. Rev. A **83**, 062116 (2011).
- [15] M. Lu, Y. Xia, L. T. Shen, J. Song, and N. B. An, Phys. Rev. A **89**, 012326 (2014).
- [16] T. Sleator and H. Weinfurter, Phys. Rev. Lett. **74**, 4087 (1995).
- [17] M. Lu, L. T. Shen, Y. Xia, and J. Song, arXiv:1305.5458v1 (2013).
- [18] B. Misra and E. C. G. Sudarshan, J. Math. Phys. **18**, 756 (1977).
- [19] Wayne M. Itano, D. J. Heinzen, J. J. Bollinger, D. J. Wineland, Phys. Rev. A **41**, 2295 (1990).
- [20] P. Kwiat, H. Weinfurter, T. Herzog, A. Zeilinger, M. A. Kasevich, Phys. Rev. Lett. **74**, 4763 (1995).
- [21] R. J. Cook, Phys. Scr. T **21**, 49 (1988).
- [22] P. Facchi and S. Pascazio, Phys. Rev. Lett. **89**, 080401 (2002).
- [23] Y. Z. Lai, J. Q. Liang, H. J. W. Müller-Kirsten, and J. G. Zhou, Phys. Rev. A **53**, 3691 (1996).
- [24] Y. Z. Lai, J. Q. Liang, H. J. W. Müller-Kirsten, and J. G. Zhou, J. Phys. A: Math. Gen. **29**, 1773 (1996).
- [25] H. R. Lewis and W. B. Riesenfeld, J. Math. Phys. **10**, 1458 (1969).
- [26] M. J. Kastoryano, F. Reiter, A. S. Sørensen, Phys. Rev. Lett, **106**, 090502 (2011).
- [27] V. S. Malinovsky and D. J. Tannor, Phys. Rev. A **56**, 4929 (1997).
- [28] U. Boscain, G. Charlot, J. P. Gauthier, S. Guérin, and H. R. Jauslin, J. Math. Phys. **43**, 2107 (2002).
- [29] I. R. Solá, V. S. Malinovsky, and D. J. Tannor, Phys. Rev. A **60**, 3081 (1999).
- [30] A. Beige, D. Braun, and P. L. Knight, New J. Phys. **2**, 22 (2000).
- [31] H. Azuma, Phys. Rev. A **68**, 022320 (2003).
- [32] R. X. Chen and L. T. Shen, Phys. Lett. A **375**, 3840 (2011).
- [33] X. B. Wang, J. Q. You, and F. Nori, Phys. Rev. A **77**, 062339 (2008).
- [34] F. T. Hioe, Phys. Rev. A **32**, 2824 (1985).
- [35] S. M. Spillane, T. J. Kippenberg, K. J. Vahala, K. W. Goh, E. Wilcut, and H. J. Kimble, Phys. Rev. A **71**, 013817 (2005).

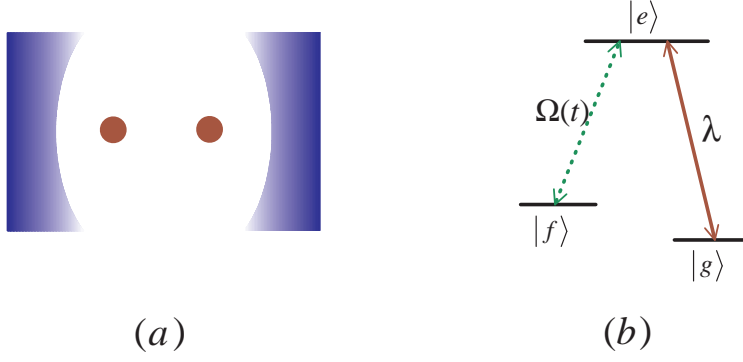


FIG. 1: (a) Cavity-atom combined system. (b) Atomic level configuration.

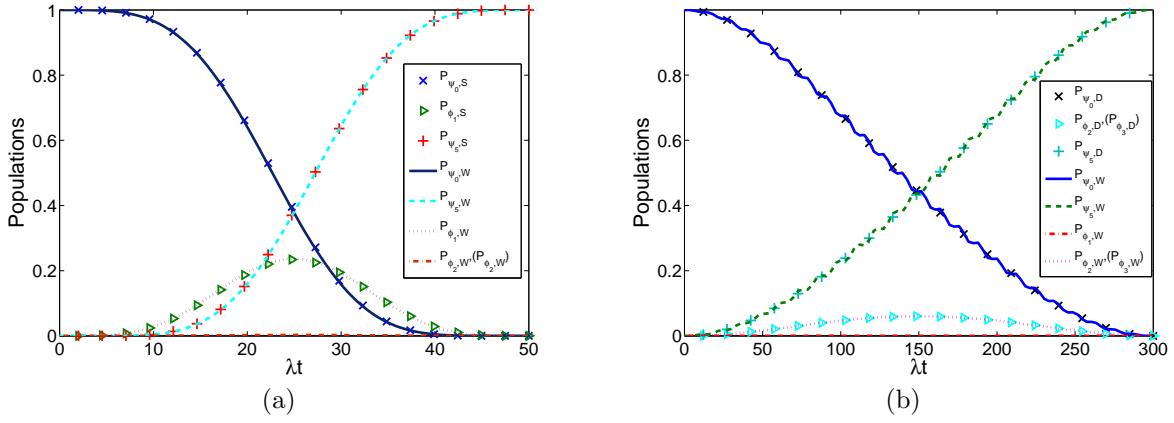


FIG. 2: (a) The comparison between the populations transfer governed by the total Hamiltonian  $H_I$  and that governed by the Hamiltonian  $H_{S_2}$  when  $\lambda t_f = 50$  and  $\epsilon = \arcsin 1/4$ . (b) The comparison between the populations transfer governed by the total Hamiltonian  $H_I$  and that governed by the dark state  $|Dark\rangle$  when  $\lambda t_f = 300$  and  $\epsilon = \arcsin 1/100$ .

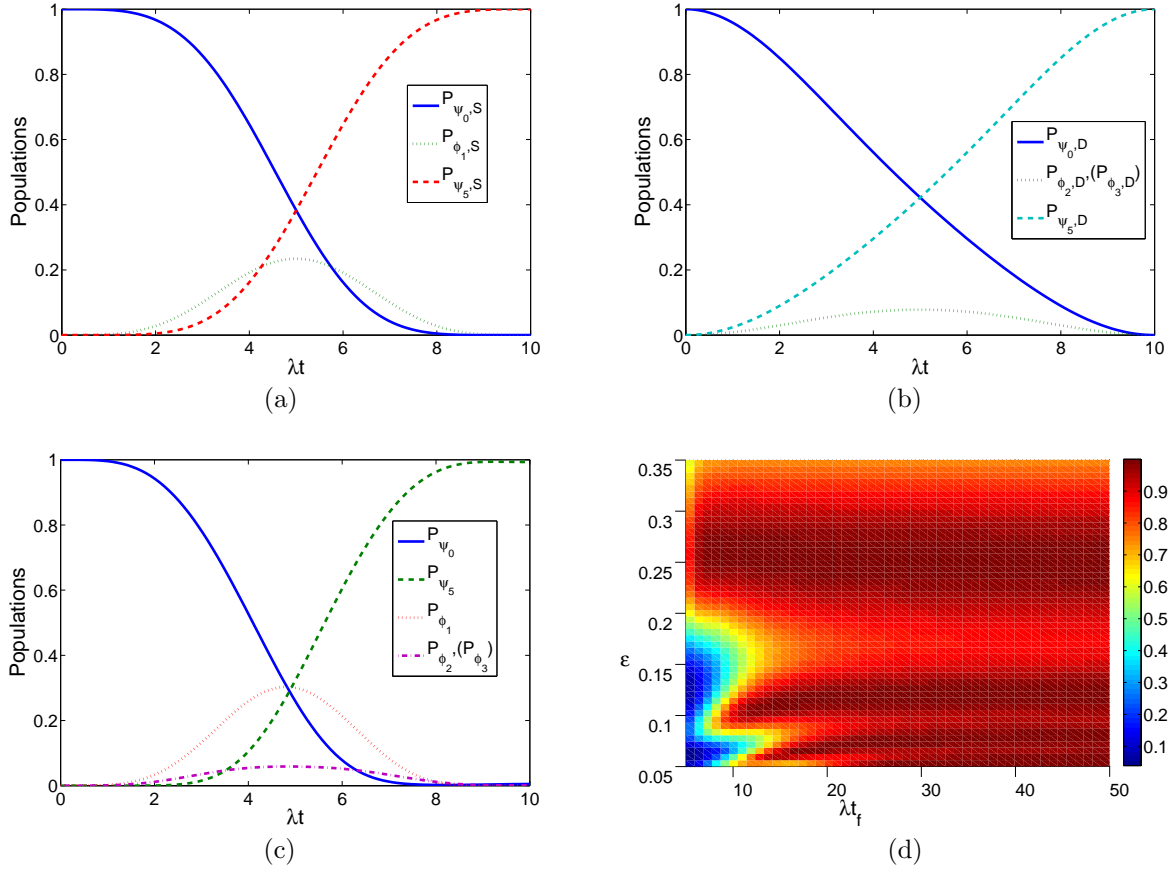


FIG. 3: (a) The time evolution of populations governed by the Hamiltonian  $H_{S_2}$  for the states  $|\psi_0\rangle$ ,  $|\phi_1\rangle$ , and  $|\psi_5\rangle$  when  $\lambda t_f = 10$  and  $\epsilon = \arcsin 0.25$ . (b) The time evolution of populations governed by the dark  $|Dark\rangle$  for the states  $|\psi_0\rangle$ ,  $|\phi_2\rangle$  ( $|\phi_3\rangle$ ), and  $|\psi_5\rangle$  when  $\lambda t_f = 10$  and  $\epsilon = \arcsin 0.25$ . (c) The time evolution of populations governed by the total Hamiltonian  $H_I$  for the states  $|\psi_0\rangle$ ,  $|\psi_5\rangle$ ,  $|\phi_1\rangle$ , and  $|\phi_2\rangle$  ( $|\phi_3\rangle$ ) when  $\lambda t_f = 10$  and  $\epsilon = \arcsin 0.25$ . (d) The fidelity  $F$  of the target state  $|\psi_5\rangle$  versus the value of  $\epsilon$  and the interaction time  $\lambda t_f$ .



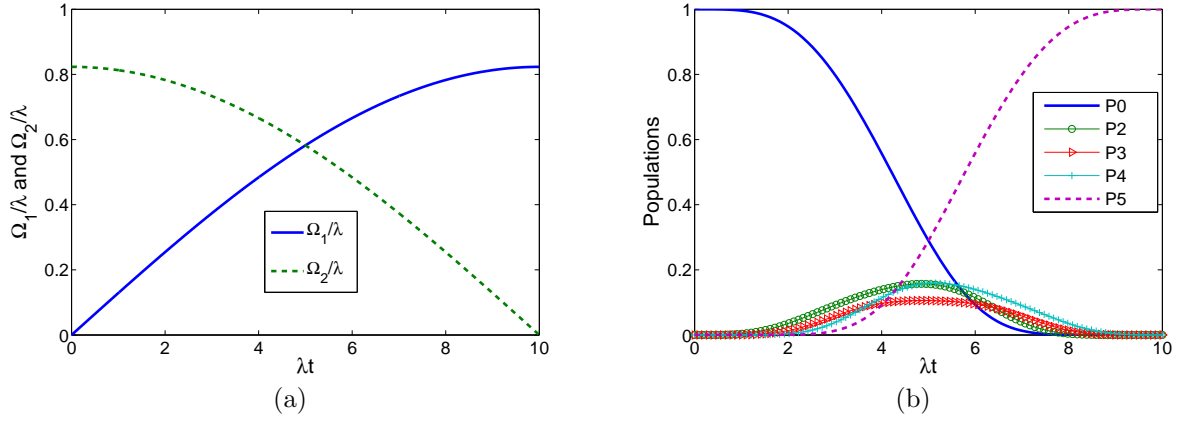


FIG. 4: (a) The time dependence of the laser fields  $\Omega_1(t)$  and  $\Omega_2(t)$  when  $\epsilon = 0.2636$  and  $\lambda t_f = 10$ . (b) Time evolution of the populations for the states  $|\psi_0\rangle$ ,  $|\psi_2\rangle$ ,  $|\psi_3\rangle$ ,  $|\psi_4\rangle$ , and  $|\psi_5\rangle$  when  $\epsilon = 0.2636$  and  $\lambda t_f = 10$ .

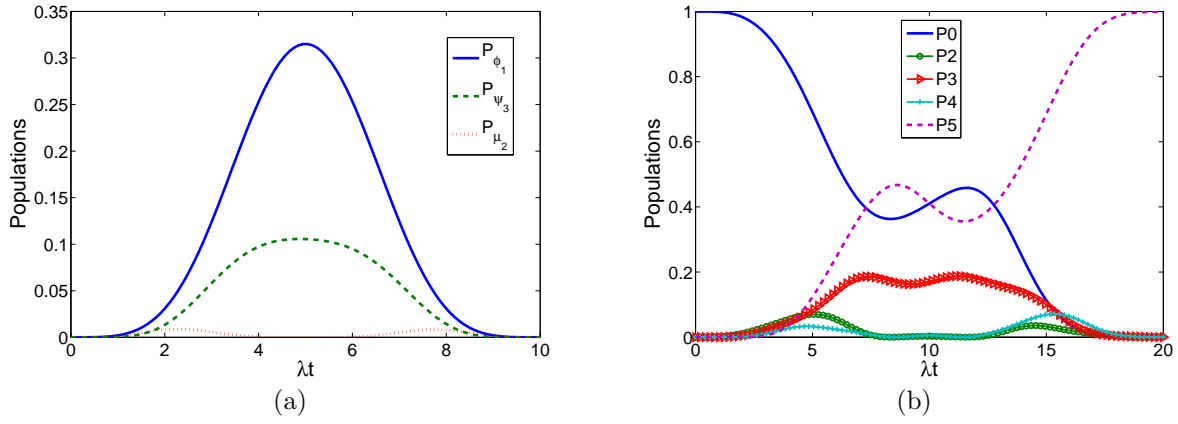


FIG. 5: (a) Time evolution of the populations for the intermediate states  $|\phi_1\rangle$ ,  $|\psi_3\rangle$ , and  $|\mu_2\rangle$  when  $\epsilon = 0.2636$  and  $\lambda t_f = 10$ . (b) Time evolution of the populations for the states  $|\psi_0\rangle$ ,  $|\psi_2\rangle$ ,  $|\psi_3\rangle$ ,  $|\psi_4\rangle$ , and  $|\psi_5\rangle$  when  $\epsilon = 0.1196$  and  $\lambda t_f = 20$ .

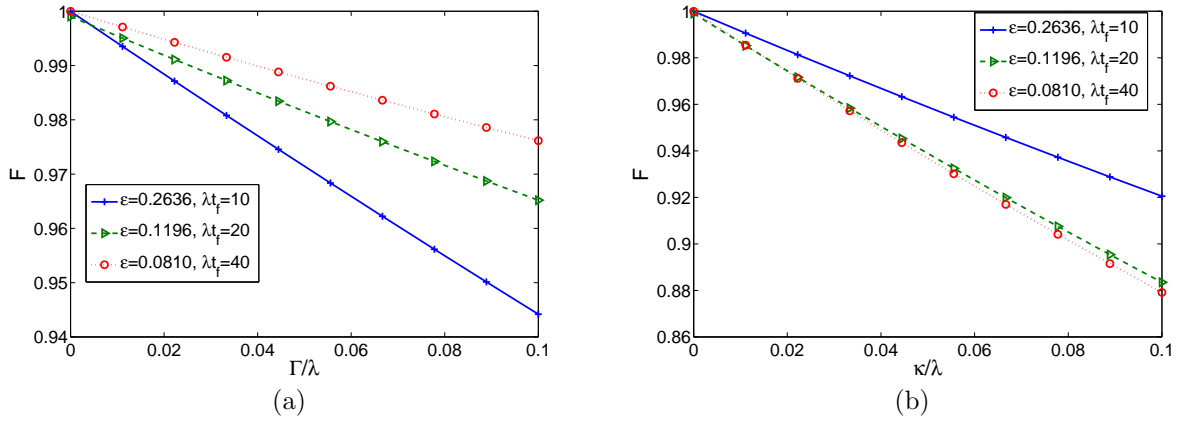


FIG. 6: (a) The influence of spontaneous emission  $\Gamma/\lambda$  on the fidelity  $F$  of the target state  $|\psi_5\rangle$  under different conditions when the decay of cavity  $\kappa = 0$ . (b) The influence of decay of cavity  $\kappa/\lambda$  on the fidelity  $F$  of the target state  $|\psi_5\rangle$  under different conditions when the spontaneous emission  $\Gamma = 0$ .

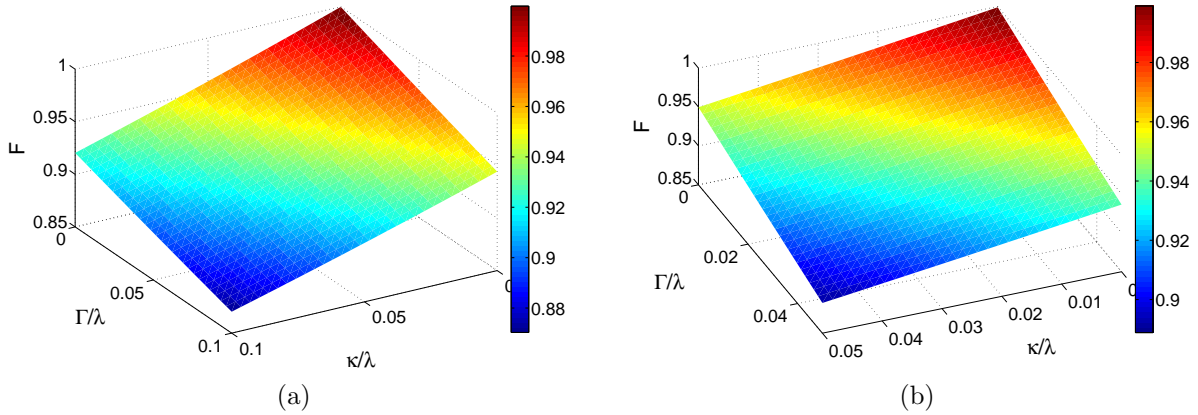


FIG. 7: (a) The fidelity  $F$  of the target state  $|\psi_5\rangle$  versus the ratios  $\Gamma/\lambda$  and  $\kappa/\lambda$  in the two-atom system. (b) The fidelity  $F$  of the target state  $|\varphi_7\rangle$  versus the ratios  $\Gamma/\lambda$  and  $\kappa/\lambda$  in the three-atom system.

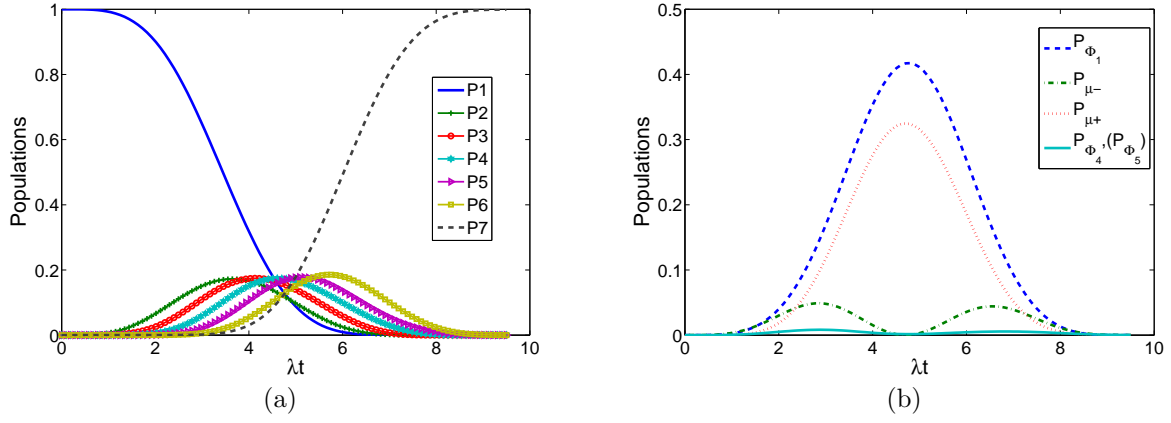


FIG. 8: (a) Time evolution of the populations for the states  $|\varphi_1\rangle - |\varphi_7\rangle$  when  $\epsilon = 0.2596$  and  $\lambda t_f = 9.5$ . (b) Time evolution of the populations for the states  $|\Phi_1\rangle$ ,  $|\mu_+\rangle$ ,  $|\mu_-\rangle$ , and  $|\Phi_4\rangle(|\Phi_5\rangle)$  when  $\epsilon = 0.2596$  and  $\lambda t_f = 9.5$ .